

Tighter sum uncertainty relations via metric-adjusted skew information

Hui Li,¹ Ting Gao,^{1,*} and Fengli Yan^{2,†}

¹*School of Mathematical Sciences, Hebei Normal University, Shijiazhuang 050024, China*

²*College of Physics, Hebei Key Laboratory of Photophysics Research and Application, Hebei Normal University, Shijiazhuang 050024, China*

We investigate the sum uncertainty relations based on metric-adjusted skew information. By means of the norm property, we propose new uncertainty relations for arbitrary finite n observables and arbitrary finite N quantum channels via metric-adjusted skew information. Since Wigner-Yanase-Dyson skew information and Wigner-Yanase skew information are two special kinds of metric-adjusted skew information, our results are applicable to the above two special cases. The uncertainty relations obtained by us are tighter than the existing ones. Detailed examples are given.

PACS numbers: 03.65.-w, 03.65.Ta

Keywords: sum uncertainty relation, metric-adjusted skew information, observable, quantum channel

I. INTRODUCTION

Uncertainty principle as a quintessential manifestation of quantum mechanics reveals the insights into the difference between quantum theory and classical theory. Heisenberg first came up with the uncertainty principle [1] in 1927, which states that it is impossible to prepare a quantum particle for both position and momentum being sharply defined. Since then, the quantitative characterization of the uncertainty relation has received extensive attention, and many results have been obtained.

There are a host of methods to characterize the uncertainty principle, one of which is variance. Lower bounds were proved to exist for the product of variances of two noncommuting observables by Robertson [2] and Schrödinger [3]. Subsequently, Maccone and Pati provided stronger uncertainty relations for all incompatible observables [4]. The stronger uncertainty relations have been tested experimentally [5]. Later, some tighter uncertainty relations with respect to variance were given [6–9].

The other well known method of characterizing uncertainty relation is entropy. Deutsch [10] first proposed a quantitative expression of the uncertainty principle by entropy for any two noncommuting observables, and the result was improved by Maassen and Uffink [11] in 1988. Furthermore, various uncertainty relations relating to different entropies were put forward [12–15]. The uncertainty relations of entropy have been shown to be a powerful tool in the field of quantum information theory ranging from quantum key distribution [16, 17], entanglement witnesses [18, 19], quantum teleportation [20], quantum steering [21] to quantum metrology [22].

Recently, Luo [23] confirmed that skew information is an alternative approach to characterize the Heisenberg uncertainty principle. In [24], Wigner and Yanase introduced skew information

$$I_\rho(A) = -\frac{1}{2}\text{Tr}[\sqrt{\rho}, A]^2 = \frac{1}{2}\|[\sqrt{\rho}, A]\|^2. \quad (1)$$

Here ρ and A represent the quantum state and the observable, respectively. The Wigner-Yanase skew information quantifies the information content of a quantum state ρ with regard to the observables not commuting with the conserved quantity. Later, a more general quantity was proposed by Dyson,

$$I_\rho^\alpha(A) = -\frac{1}{2}\text{Tr}[\rho^\alpha, A][\rho^{1-\alpha}, A], \quad 0 < \alpha < 1, \quad (2)$$

which is so-called the Wigner-Yanase-Dyson skew information, and its convexity on quantum states was resolved by Lieb and Ruskai [25, 26].

Skew information plays an important role in quantifying quantum uncertainty. First of all, the skew information can be considered as a measure because it satisfies all the expected requirements of an information measure [24]. Meanwhile, it is comparable, and sometimes better than usual variance. For the pure state, the skew information is

*Electronic address: gaoting@hebtu.edu.cn

†Electronic address: fyan@hebtu.edu.cn

the same as the variance [27], but they differ in mixed states. The remarkable difference of skew information from variance is that it is convex on quantum state space whereas the variance is concave [27]. Compared with variance, the skew information can capture more quantum nature.

Furthermore, the intrinsic relation between skew information and quantum Fisher information has been revealed [28, 29]. Quantum Fisher information is also called monotone metric which was introduced by Petz [30] and the Wigner-Yanase-Dyson metric is connected to quantum Fisher information as a special case. After that, Hansen further developed the notion of monotone metric, so-called metric-adjusted skew information [31]. The Wigner-Yanase-Dyson skew information is also connected to the metric-adjusted skew information as a special case. We will recall the metric-adjusted skew information in Sec. II.

The sum of quantum uncertainty is crucial, because it can help us to detect quantum entanglement [32–36]. To this end, the sum of quantum Fisher information defined by symmetric logarithmic derivative may be superior than the Wigner-Yanase skew information [34] as in quantum Cramér-Rao inequality. Therefore, it is of great necessity to investigate the sum uncertainty relations for all metric-adjusted skew information.

Quantum channel plays an essential role in quantum theory. The uncertainty relations for quantum channels have been extensively investigated. Ones studied the uncertainty relations in terms of Wigner-Yanase skew information for arbitrary finite N quantum channels [37, 38]. Recently, some scholars generalized the uncertainty inequalities to metric-adjusted skew information for arbitrary finite N quantum channels [39, 40].

This article is structured as follows. In Sec. II, we review the notion of metric-adjusted skew information. In Sec. III, we consider uncertainty relations for finite n observables with respect to metric-adjusted skew information. The uncertainty relations for finite N quantum channels based on metric-adjusted skew information are discussed in Sec. IV. The above results are suitable to Wigner-Yanase-Dyson skew information and Wigner-Yanase skew information. We also give some examples and compare the lower bounds obtained by us with the lower bounds in [40]. This shows that our results are more accurate than the ones in [40]. We conclude with a summary in Sec. V.

II. METRIC-ADJUSTED SKEW INFORMATION

Let $M_n(\mathbb{C})$ and \mathcal{M}_n denote the sets of all complex $n \times n$ matrices and all positive definite $n \times n$ matrices of trace 1, respectively. Suppose that for every $A, B \in M_n(\mathbb{C})$, $\rho \in \mathcal{M}_n$, and $n \in \mathbb{N}$, there is a complex number $K_\rho(A, B)$. $K_\rho(\cdot, \cdot) : M_n(\mathbb{C}) \times M_n(\mathbb{C}) \mapsto \mathbb{C}$ is called a symmetric monotone metric [30] if it satisfies

- (a) $(A, B) \mapsto K_\rho(A, B)$ is sesquilinear, that is, the function $K_\rho(A, \cdot)$ is linear and $K_\rho(\cdot, B)$ conjugate linear for every $A, B \in M_n(\mathbb{C})$.
- (b) $K_\rho(A, A) \geq 0$, and the equality holds if and only if $A = 0$.
- (c) $\rho \mapsto K_\rho(A, A) \geq 0$ is continuous on \mathcal{M}_n for every A .
- (d) $K_{T(\rho)}[T(A), T(A)] \leq K_\rho(A, A)$ for every stochastic mapping $T : M_n(\mathbb{C}) \rightarrow M_m(\mathbb{C})$ and for every $\rho \in \mathcal{M}_n$ and every A . A linear mapping $T : M_n(\mathbb{C}) \rightarrow M_m(\mathbb{C})$ is called stochastic mapping if $T(\mathcal{M}_n) \subset \mathcal{M}_m$ and T is a completely positive. In particular, such a T is trace preserving.
- (e) $K_\rho(A, B) = K_\rho(A^\dagger, B^\dagger)$.

It has been proved that there is a one-to-one correspondence between the symmetric monotone metrics and the set of functions $f : R_+ \mapsto R_+$ satisfying

- (i) f is an operator monotone, i.e., $A \geq B$ implies $f(A) \geq f(B)$ for any positive invertible matrices A, B .
- (ii) $tf(t^{-1}) = f(t)$ for all $t \geq 0$.

Here R_+ is the set of all positive real number. It is shown that if $K_\rho(\cdot, \cdot)$ satisfies $K_{I/n}(I, I) = 1$, then the associated normalizing condition on the function f needs to satisfy $f(1) = 1$. Here I is n -dimension identity operator.

The symmetric monotone metrics $K_\rho(A, B)$ can be expressed in the following form

$$K_\rho(A, B) = \text{Tr}[A^\dagger c(L_\rho, R_\rho)B], \quad (3)$$

where c is so-called Morozova-Chentsov function and $c(L_\rho, R_\rho)$ is the function taken in the pair of commuting left and right multiplication operators (denote L_ρ and R_ρ , respectively). The Morozova-Chentsov function is given in the form

$$c(x, y) = \frac{1}{yf(xy^{-1})}, \quad x, y > 0, \quad (4)$$

where f is a function satisfying (i) and (ii). When the associated Morozova-Chentsov functions, respectively, are chosen as

$$c^{\text{WY}}(x, y) = \frac{4}{(\sqrt{x} + \sqrt{y})^2}, \quad x, y > 0, \quad (5)$$

and

$$c^\alpha(x, y) = \frac{1}{\alpha(1-\alpha)} \frac{(x^\alpha - y^\alpha)(x^{1-\alpha} - y^{1-\alpha})}{(x-y)^2}, \quad 0 < \alpha < 1, \quad (6)$$

the monotone metrics

$$K_\rho^{\text{WY}}(A, B) = \text{Tr}[A^\dagger c_\rho^{\text{WY}}(L_\rho, R_\rho)B], \quad (7)$$

and

$$K_\rho^\alpha(A, B) = \text{Tr}[A^\dagger c_\rho^\alpha(L_\rho, R_\rho)B], \quad (8)$$

are called the Wigner-Yanase metric and the Wigner-Yanase-Dyson metric, respectively. In addition, a symmetric monotone metric on the state space of a quantum system is regular [31], if the corresponding Morozova-Chentsov function c admits

$$m(c) = \lim_{t \rightarrow 0} c(t, 1)^{-1} > 0. \quad (9)$$

$m(c)$ is called the metric constant and $m(c) = f(0)$.

In [31], Hansen introduced the metric-adjusted skew information $I_\rho^c(A)$ by symmetric monotone metric

$$\begin{aligned} I_\rho^c(A) &= \frac{m(c)}{2} K_\rho^c(\text{i}[\rho, A], \text{i}[\rho, A]) \\ &= \frac{m(c)}{2} \text{Tr} \{ \text{i}[\rho, A] c(L_\rho, R_\rho) \text{i}[\rho, A] \} \end{aligned} \quad (10)$$

for every $\rho \in \mathcal{M}_n$ and every self-adjoint $A \in M_n(\mathbb{C})$, where c is the Morozova-Chentsov function of a regular metric. Since the commutator $\text{i}[\rho, A] = \text{i}(L_\rho - R_\rho)A$, the metric-adjusted skew information can be rewritten as

$$\begin{aligned} I_\rho^c(A) &= \frac{m(c)}{2} \text{Tr} \{ A(\text{i}(L_\rho - R_\rho))^\dagger c(L_\rho, R_\rho) \text{i}(L_\rho - R_\rho)A \} \\ &= \frac{m(c)}{2} \text{Tr} \{ A \hat{c}(L_\rho, R_\rho) A \}, \end{aligned} \quad (11)$$

where $\hat{c}(x, y) = (x - y)^2 c(x, y)$, $x, y > 0$.

If we consider the Wigner-Yanase-Dyson metric with Morozova-Chentsov function (6), then the metric constant $m(c^\alpha) = \alpha(1-\alpha)$ and the metric-adjusted skew information,

$$\begin{aligned} I_\rho^{c^\alpha}(A) &= \frac{\alpha(1-\alpha)}{2} \text{Tr} \{ \text{i}[\rho, A] c^\alpha(L_\rho, R_\rho) \text{i}[\rho, A] \} \\ &= -\frac{1}{2} \text{Tr}[\rho^\alpha, A] [\rho^{1-\alpha}, A] \end{aligned} \quad (12)$$

being the Wigner-Yanase-Dyson skew information $I_\rho^\alpha(A)$.

When $\alpha = \frac{1}{2}$, $I_\rho^\alpha(A)$ becomes Wigner-Yanase skew information $I_\rho(A) = -\frac{1}{2} \text{Tr}[\sqrt{\rho}, A]^2$.

III. UNCERTAINTY RELATIONS FOR FINITE OBSERVABLES BASED ON METRIC-ADJUSTED SKEW INFORMATION

In this section, we present two sum uncertainty relations via metric-adjusted skew information for arbitrary n observables, and the results also hold based on Wigner-Yanase-Dyson skew information and Wigner-Yanase skew information. Then we provide two examples which show that our results are better than existing ones.

For finite n observables A_1, A_2, \dots, A_n ($n > 2$), Cai showed the sum uncertainty relations with respect to metric-adjusted skew information [39],

$$\sum_{i=1}^n I_\rho^c(A_i) \geq \frac{1}{n-2} \left[\sum_{1 \leq i < j \leq n} I_\rho^c(A_i + A_j) - \frac{1}{(n-1)^2} \left(\sum_{1 \leq i < j \leq n} \sqrt{I_\rho^c(A_i + A_j)} \right)^2 \right]. \quad (13)$$

Recently, Ren *et al.* formulated a following uncertainty inequality [40]

$$\sum_{i=1}^n I_\rho^c(A_i) \geq \frac{1}{n} I_\rho^c \left(\sum_{i=1}^n A_i \right) + \frac{2}{n^2(n-1)} \left(\sum_{1 \leq i < j \leq n} \sqrt{I_\rho^c(A_i - A_j)} \right)^2. \quad (14)$$

Here A_1, A_2, \dots, A_n ($n \geq 2$) are observables. For simplicity, the lower bounds in (13) and (14) are marked by LB_1 and LB_2 , respectively.

In [38], Zhang *et al.* introduced two inequalities which play an essential role in this paper, so we take the inequalities as a Lemma.

Lemma 1 [38]. Let \mathbf{a}_i be vectors in a Hilbert space, then

$$\sum_{i=1}^n \|\mathbf{a}_i\|^2 \geq \frac{1}{2n-2} \left[\frac{2}{n(n-1)} \left(\sum_{1 \leq i < j \leq n} \|\mathbf{a}_i + \mathbf{a}_j\| \right)^2 + \sum_{1 \leq i < j \leq n} \|\mathbf{a}_i - \mathbf{a}_j\|^2 \right], \quad (15)$$

and

$$\sum_{i=1}^n \|\mathbf{a}_i\|^2 \geq \frac{1}{2n-2} \left[\frac{2}{n(n-1)} \left(\sum_{1 \leq i < j \leq n} \|\mathbf{a}_i - \mathbf{a}_j\| \right)^2 + \sum_{1 \leq i < j \leq n} \|\mathbf{a}_i + \mathbf{a}_j\|^2 \right], \quad (16)$$

where $\|\cdot\|$ stands for the norm of a vector.

Note that the inequalities have the following relation

$$\begin{aligned} \sum_{i=1}^n \|\mathbf{a}_i\|^2 &\geq \frac{1}{2n-2} \left[\frac{2}{n(n-1)} \left(\sum_{1 \leq i < j \leq n} \|\mathbf{a}_i - \mathbf{a}_j\| \right)^2 + \sum_{1 \leq i < j \leq n} \|\mathbf{a}_i + \mathbf{a}_j\|^2 \right] \\ &\geq \frac{1}{n} \left\| \sum_{i=1}^n \mathbf{a}_i \right\|^2 + \frac{2}{n^2(n-1)} \left(\sum_{1 \leq i < j \leq n} \|\mathbf{a}_i - \mathbf{a}_j\| \right)^2. \end{aligned} \quad (17)$$

This inequality is helpful for us to explore the tighter uncertainty relation.

In [38], the authors given two sum uncertainty relations based on Wigner-Yanase skew information, which can be extended to all the metric-adjusted skew information by the definition of the symmetric monotone metrics. Next, we give the tighter sum uncertainty relations with respect to metric-adjusted skew information in the following Theorem.

Theorem 1. Let A_1, A_2, \dots, A_n ($n \geq 2$) be arbitrary n observables. Then the sum uncertainty relations with respect to metric-adjusted skew information are of the form

$$\sum_{i=1}^n I_\rho^c(A_i) \geq \frac{1}{2n-2} \left\{ \frac{2}{n(n-1)} \left(\sum_{1 \leq i < j \leq n} \sqrt{I_\rho^c(A_i + A_j)} \right)^2 + \sum_{1 \leq i < j \leq n} I_\rho^c(A_i - A_j) \right\}, \quad (18)$$

and

$$\sum_{i=1}^n I_\rho^c(A_i) \geq \frac{1}{2n-2} \left\{ \frac{2}{n(n-1)} \left(\sum_{1 \leq i < j \leq n} \sqrt{I_\rho^c(A_i - A_j)} \right)^2 + \sum_{1 \leq i < j \leq n} I_\rho^c(A_i + A_j) \right\}. \quad (19)$$

Specially, the inequality can be saturated when $n = 2$, i.e.,

$$I_\rho^c(A_1) + I_\rho^c(A_2) = \frac{1}{2} [I_\rho^c(A_1 + A_2) + I_\rho^c(A_1 - A_2)]. \quad (20)$$

Proof. Obviously the lower bound of inequality (18) is nonnegative. Because the symmetric monotone metrics $K_\rho^c(\cdot, \cdot)$ meet with the property of norm. According to Lemma 1, we have

$$\begin{aligned} \sum_{i=1}^n K_\rho^c(\mathbf{i}[\rho, A_i], \mathbf{i}[\rho, A_i]) &\geq \frac{1}{2n-2} \left\{ \frac{2}{n(n-1)} \left(\sum_{1 \leq i < j \leq n} \sqrt{K_\rho^c(\mathbf{i}[\rho, A_i + A_j], \mathbf{i}[\rho, A_i + A_j])} \right)^2 \right. \\ &\quad \left. + \sum_{1 \leq i < j \leq n} K_\rho^c(\mathbf{i}[\rho, A_i - A_j], \mathbf{i}[\rho, A_i - A_j]) \right\}. \end{aligned} \quad (21)$$

Both sides of this formula multiply by a constant $\frac{f(0)}{2}$, then we get the inequality (18) easily.

Using the similar procedure, we can get the inequality (19). \blacksquare

For convenience, the lower bounds in (18) and (19) are marked by LB_3 and LB_4 , respectively.

It is acknowledged that different results can be obtained by taking different Morozova-Chentsov functions for metric-adjusted skew information. We consider a special case which is the Wigner-Yanase-Dyson metric with the Morozova-Chentsov function (6). In this condition, the metric-adjusted skew information $I_\rho^c(A)$ becomes Wigner-Yanase-Dyson skew information $I_\rho^\alpha(A)$.

Corollary 1. Let A_1, A_2, \dots, A_n ($n \geq 2$) be arbitrary n observables. Then the sum uncertainty relations relating to Wigner-Yanase-Dyson skew information are given in the form

$$\sum_{i=1}^n I_\rho^\alpha(A_i) \geq \frac{1}{2n-2} \left\{ \frac{2}{n(n-1)} \left(\sum_{1 \leq i < j \leq n} \sqrt{I_\rho^\alpha(A_i + A_j)} \right)^2 + \sum_{1 \leq i < j \leq n} I_\rho^\alpha(A_i - A_j) \right\}, \quad (22)$$

and

$$\sum_{i=1}^n I_\rho^\alpha(A_i) \geq \frac{1}{2n-2} \left\{ \frac{2}{n(n-1)} \left(\sum_{1 \leq i < j \leq n} \sqrt{I_\rho^\alpha(A_i - A_j)} \right)^2 + \sum_{1 \leq i < j \leq n} I_\rho^\alpha(A_i + A_j) \right\}. \quad (23)$$

Specially, the inequality can be saturated when $n = 2$.

Wigner-Yanase-Dyson skew information becomes Wigner-Yanase skew information when $\alpha = \frac{1}{2}$, it is consistent with the results in [38]. Therefore, the conclusions drawn by us cover the ones in [38].

Next we present two examples in term of Wigner-Yanase-Dyson skew information.

Example 1. For one-qubit state $\rho = \frac{I + \vec{r} \cdot \vec{\sigma}}{2}$ with Bloch vector $\vec{r} = (\frac{\sqrt{3}}{2} \cos \theta, \frac{\sqrt{3}}{2} \sin \theta, 0)$, we regard Pauli operators $\sigma_x, \sigma_y, \sigma_z$ as observables. The lower bounds of the sum uncertainty relations based on Wigner-Yanase-Dyson skew information are illustrated in FIG. 1(a). The difference value between our lower bound LB_4 and the lower bound LB_2 is illustrated in FIG. 1(b). One can obviously see that the lower bound LB_4 is larger than the lower bound LB_2 . Considering a special case, we take $\alpha = \frac{1}{3}$. The lower bounds of the sum uncertainty relations are illustrated in FIG. 1(c). Since we know the lower bound LB_2 is always larger than the lower bound LB_1 from FIG. 1(a), we only discuss the lower bounds LB_4, LB_3, LB_2 here. The lower bound LB_4 is greater for some cases, while the lower bound LB_3 is superior for some cases.

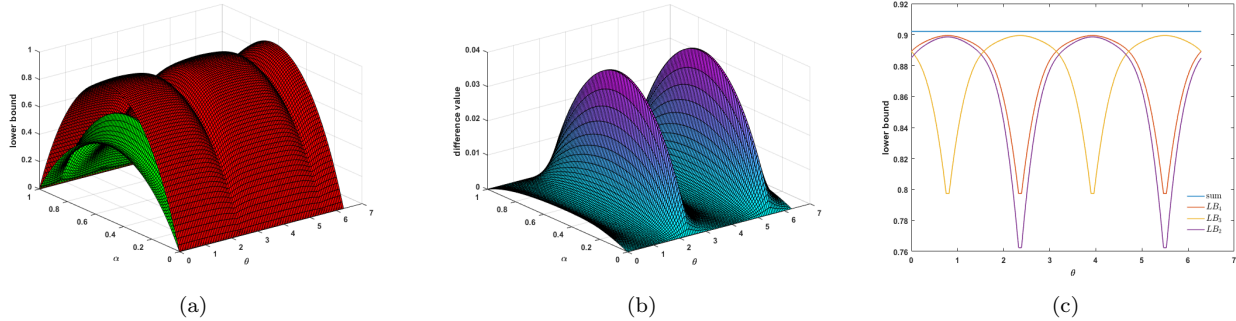


FIG. 1: In (a), compared with the lower bounds for one-qubit ρ . The red surface and the green surface represent respectively the lower bounds LB_2, LB_1 for arbitrary α . The (b) represents the difference value between our lower bound LB_4 and the lower bound LB_2 . Obviously, the lower bound LB_4 is the tightest among the lower bounds LB_1, LB_2 , and LB_4 . Specially, in (c), we fix $\alpha = \frac{1}{3}$. The blue line represents the sum of uncertainty relation in term of Wigner-Yanase-Dyson skew information; the red line represents the lower bound LB_4 ; the yellow line represents the lower bound LB_3 ; the purple line represents the lower bound LB_2 . One sees that the lower bound LB_4 is larger than the lower bound LB_2 . The larger the lower bounds LB_4 and LB_2 are, the smaller the lower bound LB_3 is. Conversely, the smaller the lower bounds LB_4 and LB_2 are, the larger the lower bound LB_3 is.

Example 2. For a Gisin state $\rho = \lambda |\psi(\theta)\rangle\langle\psi(\theta)| + (1 - \lambda)\sigma_0$, where $|\psi(\theta)\rangle = \sin\theta|01\rangle - \cos\theta|10\rangle$, $\sigma_0 = \frac{1}{2}|00\rangle\langle 00| + \frac{1}{2}|11\rangle\langle 11|$, $0 \leq \lambda \leq 1$, and $0 \leq \theta \leq 2\pi$, we view operators $I \otimes \sigma_x, I \otimes \sigma_y, I \otimes \sigma_z$ as observables. We take $\alpha = \frac{1}{3}$, the lower bounds of the sum uncertainty relations in terms of Wigner-Yanase-Dyson skew information are illustrated in FIG. 2. It is apparent that the lower bounds LB_3 and LB_4 are larger than the lower bound LB_1 and LB_2 .

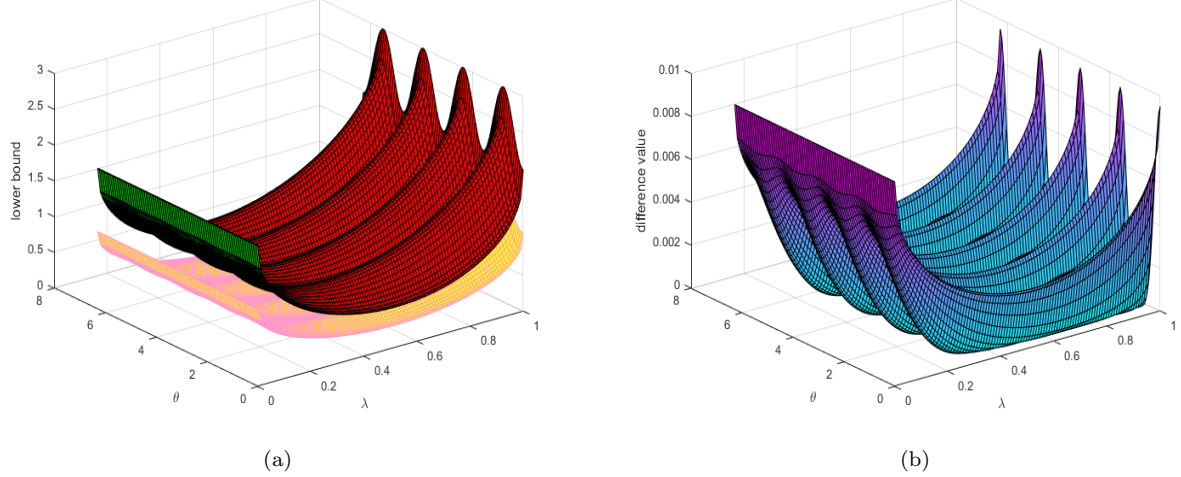


FIG. 2: The comparison of different lower bounds for Gisin state ρ . In (a), we fix $\alpha = \frac{1}{3}$. The red surface represents the lower bounds LB_3 and LB_4 , the green surface in middle and the yellow surface represent respectively the lower bounds LB_2 and LB_1 . Obviously, the lower bounds we obtained are larger. The (b) represents the difference value between our lower bounds LB_3 or LB_4 and the lower bound LB_2 .

IV. UNCERTAINTY RELATIONS FOR FINITE QUANTUM CHANNELS BASED ON METRIC-ADJUSTED SKEW INFORMATION

In this section, we give new uncertainty relations for arbitrary N quantum channels in terms of metric-adjusted skew information, and the results also hold with respect to Wigner-Yanase-Dyson skew information and Wigner-Yanase skew information. We also provide two examples for the sake of illustrating our results.

Given a quantum state ρ and a quantum channel Φ with Kraus representation $\Phi(\rho) = \sum_i K_i \rho K_i^\dagger$. In [39], Cai gave an uncertainty quantification of quantum channels Φ based on metric-adjusted skew information

$$I_\rho^c(\Phi) = \sum_i I_\rho^c(K_i), \quad (24)$$

where

$$\begin{aligned} I_\rho^c(K_i) &= \frac{m(c)}{2} K_\rho^c(i[\rho, K_i], i[\rho, K_i]) \\ &= \frac{m(c)}{2} \text{Tr} \left\{ i[\rho, K_i^\dagger] c(L_\rho, R_\rho) i[\rho, K_i] \right\}. \end{aligned} \quad (25)$$

The special case for Wigner-Yanase-Dyson metric with the Morozova-Chenstov function (6), analogously, the metric-adjusted skew information of quantum channels $I_\rho^c(\Phi)$ reduces to the Wigner-Yanase-Dyson skew information $I_\rho^\alpha(\Phi)$, the expression is of the form

$$I_\rho^{c^\alpha}(\Phi) = \sum_i I_\rho^{c^\alpha}(K_i) = -\frac{1}{2} \sum_i \text{Tr}[\rho^\alpha, K_i^\dagger][\rho^{1-\alpha}, K_i]. \quad (26)$$

When $\alpha = \frac{1}{2}$, $I_\rho^\alpha(\Phi)$ becomes the Wigner-Yanase skew information associated with quantum channels,

$$I_\rho(\Phi) = \sum_i I_\rho(K_i) = -\frac{1}{2} \sum_i \text{Tr}[\sqrt{\rho}, K_i^\dagger][\sqrt{\rho}, K_i]. \quad (27)$$

For arbitrary N quantum channels $\Phi_1, \Phi_2, \dots, \Phi_N$ ($N \geq 2$), and each channel has Kraus representation $\Phi_t(\rho) = \sum_{i=1}^n K_i^t \rho (K_i^t)^\dagger$, $t = 1, 2, \dots, N$. In [40], Ren *et al.* gave uncertainty quantification of quantum channels Φ based on

metric-adjusted skew information,

$$\sum_{t=1}^N I_\rho^c(\Phi_t) \geq \max_{\pi_t, \pi_s \in S_n} \frac{1}{N-2} \left\{ \sum_{1 \leq t < s \leq N} \sum_{i=1}^n I_\rho^c(K_{\pi_t(i)}^t + K_{\pi_s(i)}^s) - \frac{1}{(N-1)^2} \left[\sum_{i=1}^n \left(\sum_{1 \leq t < s \leq N} \sqrt{I_\rho^c(K_{\pi_t(i)}^t + K_{\pi_s(i)}^s)} \right)^2 \right] \right\}, \quad (28)$$

and

$$\sum_{t=1}^N I_\rho^c(\Phi_t) \geq \max_{\pi_t, \pi_s \in S_n} \left\{ \frac{1}{N} \sum_{i=1}^n I_\rho^c \left(\sum_{t=1}^N K_{\pi_t(i)}^t \right) + \frac{2}{N^2(N-1)} \left[\sum_{i=1}^n \left(\sum_{1 \leq t < s \leq N} \sqrt{I_\rho^c(K_{\pi_t(i)}^t - K_{\pi_s(i)}^s)} \right)^2 \right] \right\}. \quad (29)$$

The inequality (28) holds for $N > 2$, while the inequality (29) holds for $N \geq 2$. For simplicity, the lower bounds in (28) and (29) are marked by \overline{LB}_1 and \overline{LB}_2 , respectively.

Next, we will present two sum uncertainty relations for arbitrary finite N quantum channels in terms of metric-adjusted skew information.

Theorem 2. Let $\Phi_1, \Phi_2, \dots, \Phi_N$ ($N \geq 2$) be arbitrary N quantum channels, and each channel has Kraus representation $\Phi_t(\rho) = \sum_{i=1}^n K_i^t \rho (K_i^t)^\dagger$, $t = 1, 2, \dots, N$, we have

$$\sum_{t=1}^N I_\rho^c(\Phi_t) \geq \max_{\pi_t, \pi_s \in S_n} \frac{1}{2N-2} \left\{ \frac{2}{N(N-1)} \left[\sum_{i=1}^n \left(\sum_{1 \leq t < s \leq N} \sqrt{I_\rho^c(K_{\pi_t(i)}^t + K_{\pi_s(i)}^s)} \right)^2 \right] + \sum_{1 \leq t < s \leq N} \sum_{i=1}^n I_\rho^c(K_{\pi_t(i)}^t - K_{\pi_s(i)}^s) \right\}, \quad (30)$$

and

$$\sum_{t=1}^N I_\rho^c(\Phi_t) \geq \max_{\pi_t, \pi_s \in S_n} \frac{1}{2N-2} \left\{ \frac{2}{N(N-1)} \left[\sum_{i=1}^n \left(\sum_{1 \leq t < s \leq N} \sqrt{I_\rho^c(K_{\pi_t(i)}^t - K_{\pi_s(i)}^s)} \right)^2 \right] + \sum_{1 \leq t < s \leq N} \sum_{i=1}^n I_\rho^c(K_{\pi_t(i)}^t + K_{\pi_s(i)}^s) \right\}, \quad (31)$$

where $\pi_t, \pi_s \in S_n$ is an arbitrary n -element permutation.

Proof. According to the norm inequality of Lemma 1, we can get

$$\sum_{t=1}^N I_\rho^c(K_{\pi_t(i)}^t) \geq \frac{1}{2N-2} \left\{ \frac{2}{N(N-1)} \left(\sum_{1 \leq t < s \leq N} \sqrt{I_\rho^c(K_{\pi_t(i)}^t + K_{\pi_s(i)}^s)} \right)^2 + \sum_{1 \leq t < s \leq N} I_\rho^c(K_{\pi_t(i)}^t - K_{\pi_s(i)}^s) \right\}, \quad (32)$$

both sides of this formula sum over i , we have the inequality (30).

Using the similar method, we can get the inequality (31). For simplicity, the lower bounds in (30) and (31) are marked by \overline{LB}_3 and \overline{LB}_4 , respectively. \blacksquare

The results about channels can also apply to Wigner-Yanase-Dyson skew information, so we can get the following conclusions.

Corollary 2. Let $\Phi_1, \Phi_2, \dots, \Phi_N$ ($N \geq 2$) be arbitrary N quantum channels, and each channel has Kraus representation $\Phi_t(\rho) = \sum_{i=1}^n K_i^t \rho (K_i^t)^\dagger$, $t = 1, 2, \dots, N$, we have

$$\sum_{t=1}^N I_\rho^\alpha(\Phi_t) \geq \max_{\pi_t, \pi_s \in S_n} \frac{1}{2N-2} \left\{ \frac{2}{N(N-1)} \left[\sum_{i=1}^n \left(\sum_{1 \leq t < s \leq N} \sqrt{I_\rho^\alpha(K_{\pi_t(i)}^t + K_{\pi_s(i)}^s)} \right)^2 \right] + \sum_{1 \leq t < s \leq N} \sum_{i=1}^n I_\rho^\alpha(K_{\pi_t(i)}^t - K_{\pi_s(i)}^s) \right\}, \quad (33)$$

and

$$\begin{aligned} \sum_{t=1}^N I_\rho^\alpha(\Phi_t) &\geq \max_{\pi_t, \pi_s \in S_n} \frac{1}{2N-2} \left\{ \frac{2}{N(N-1)} \left[\sum_{i=1}^n \left(\sum_{1 \leq t < s \leq N} \sqrt{I_\rho^\alpha(K_{\pi_t(i)}^t - K_{\pi_s(i)}^s)} \right)^2 \right] \right. \\ &\quad \left. + \sum_{1 \leq t < s \leq N} \sum_{i=1}^n I_\rho^\alpha(K_{\pi_t(i)}^t + K_{\pi_s(i)}^s) \right\}, \end{aligned} \quad (34)$$

where $\pi_t, \pi_s \in S_n$ is an arbitrary n -element permutation.

When $\alpha = \frac{1}{2}$, Wigner-Yanase-Dyson skew information becomes Wigner-Yanase skew information, so we have

$$\begin{aligned} \sum_{t=1}^N I_\rho(\Phi_t) &\geq \max_{\pi_t, \pi_s \in S_n} \frac{1}{2N-2} \left\{ \frac{2}{N(N-1)} \left[\sum_{i=1}^n \left(\sum_{1 \leq t < s \leq N} \sqrt{I_\rho(K_{\pi_t(i)}^t + K_{\pi_s(i)}^s)} \right)^2 \right] \right. \\ &\quad \left. + \sum_{1 \leq t < s \leq N} \sum_{i=1}^n I_\rho(K_{\pi_t(i)}^t - K_{\pi_s(i)}^s) \right\}, \end{aligned} \quad (35)$$

and

$$\begin{aligned} \sum_{t=1}^N I_\rho(\Phi_t) &\geq \max_{\pi_t, \pi_s \in S_n} \frac{1}{2N-2} \left\{ \frac{2}{N(N-1)} \left[\sum_{i=1}^n \left(\sum_{1 \leq t < s \leq N} \sqrt{I_\rho(K_{\pi_t(i)}^t - K_{\pi_s(i)}^s)} \right)^2 \right] \right. \\ &\quad \left. + \sum_{1 \leq t < s \leq N} \sum_{i=1}^n I_\rho(K_{\pi_t(i)}^t + K_{\pi_s(i)}^s) \right\}. \end{aligned} \quad (36)$$

The following we will show two examples based on Wigner-Yanase-Dyson skew information. One is that each channel has the same number of Kraus operators, and the other is that each channel has a different number of Kraus operators.

Example 3. For one-qubit state $\rho = \frac{I+\vec{r}\cdot\vec{\sigma}}{2}$ with Bloch vector $\vec{r}=(\frac{\sqrt{3}}{2}\cos\theta, \frac{\sqrt{3}}{2}\sin\theta, 0)$, $0 \leq \theta \leq \pi$, and three channels, the bit-flipping channel Λ , the phase-flipping channel ε , and the amplitude damping channel ϕ , where $\Lambda(\rho) = \sum_{i=1}^2 E_i \rho E_i^\dagger$ with $E_1 = \sqrt{1-p}(|0\rangle\langle 0| + |1\rangle\langle 1|)$, $E_2 = \sqrt{p}(|0\rangle\langle 1| + |1\rangle\langle 0|)$, $\varepsilon(\rho) = \sum_{i=1}^2 F_i \rho F_i^\dagger$ with

$F_1 = \sqrt{1-p}(|0\rangle\langle 0| + |1\rangle\langle 1|)$, $F_2 = \sqrt{p}(|0\rangle\langle 0| - |1\rangle\langle 1|)$, $\phi(\rho) = \sum_{i=1}^2 K_i \rho K_i^\dagger$ with $K_1 = |0\rangle\langle 0| + \sqrt{1-p}|1\rangle\langle 1|$, $K_2 = \sqrt{p}|1\rangle\langle 1|$, $0 \leq p \leq 1$. Then according to Corollary 2, one has $I_\rho^\alpha(\Lambda) + I_\rho^\alpha(\varepsilon) + I_\rho^\alpha(\phi) \geq \max\{A_1, A_2, A_3, A_4\}$, and $I_\rho^\alpha(\Lambda) + I_\rho^\alpha(\varepsilon) + I_\rho^\alpha(\phi) \geq \max\{B_1, B_2, B_3, B_4\}$, where A_i, B_i ($i = 1, 2, 3, 4$) are the lower bounds corresponding to $\{\pi_1 = (1), \pi_2 = (1), \pi_3 = (1)\}$, $\{\pi_1 = (1), \pi_2 = (12), \pi_3 = (12)\}$, $\{\pi_1 = (1), \pi_2 = (1), \pi_3 = (12)\}$ or $\{\pi_1 = (1), \pi_2 = (12), \pi_3 = (1)\}$. Similarly, one can get $I_\rho^\alpha(\Lambda) + I_\rho^\alpha(\varepsilon) + I_\rho^\alpha(\phi) \geq \max\{C_1, C_2, C_3, C_4\}$ and $I_\rho^\alpha(\Lambda) + I_\rho^\alpha(\varepsilon) + I_\rho^\alpha(\phi) \geq \max\{D_1, D_2, D_3, D_4\}$ by (28) and (29), respectively. Here the C_i, D_i ($i = 1, 2, 3, 4$) are similar to A_i, B_i ($i = 1, 2, 3, 4$). Here π_i ($i = 1, 2, 3$) need to take all of the binary permutations, but the lower bounds in the case $\{\pi_1 = (1), \pi_2 = (1), \pi_3 = (1)\}$ and the case $\{\pi_1 = (12), \pi_2 = (12), \pi_3 = (12)\}$ are same, similarly the lower bounds in the cases $\{\pi_1 = (1), \pi_2 = (12), \pi_3 = (12)\}$ and $\{\pi_1 = (12), \pi_2 = (1), \pi_3 = (1)\}$, $\{\pi_1 = (1), \pi_2 = (1), \pi_3 = (12)\}$ and $\{\pi_1 = (12), \pi_2 = (12), \pi_3 = (1)\}$, $\{\pi_1 = (1), \pi_2 = (12), \pi_3 = (1)\}$ and $\{\pi_1 = (12), \pi_2 = (1), \pi_3 = (12)\}$ are same, so we only need to consider four cases. When $\alpha = \frac{1}{3}$ and $p = 0.7$, it is apparent that the lower bounds \overline{LB}_4 we obtained are always tighter than the lower bound \overline{LB}_2 , and we find for some cases the lower bounds \overline{LB}_3 and \overline{LB}_4 are greater, whereas for some cases the lower bound \overline{LB}_1 is stronger, which is illustrated in FIG. 3.

Example 4. For one-qubit state $\rho = \frac{I+\vec{r}\cdot\vec{\sigma}}{2}$ with Bloch vector $\vec{r}=(\frac{\sqrt{3}}{2}\cos\theta, \frac{\sqrt{3}}{2}\sin\theta, 0)$, $0 \leq \theta \leq \pi$, and three channels, the bit-flipping channel Λ , the phase-flipping channel ε , and one unitary channel U , respectively, where $\Lambda(\rho) = \sum_{i=1}^2 E_i \rho E_i^\dagger$ with $E_1 = \sqrt{1-p}(|0\rangle\langle 0| + |1\rangle\langle 1|)$, $E_2 = \sqrt{p}(|0\rangle\langle 1| + |1\rangle\langle 0|)$, $\varepsilon(\rho) = \sum_{i=1}^2 F_i \rho F_i^\dagger$ with $F_1 = \sqrt{1-p}(|0\rangle\langle 0| + |1\rangle\langle 1|)$, $F_2 = \sqrt{p}(|0\rangle\langle 0| - |1\rangle\langle 1|)$, and $U = \cos\frac{\pi}{8}|0\rangle\langle 0| + \sin\frac{\pi}{8}|0\rangle\langle 1| - \sin\frac{\pi}{8}|1\rangle\langle 0| + \cos\frac{\pi}{8}|1\rangle\langle 1|$. Since the number of Kraus operators in each channel are different, we adopt the method of supplementing **0** proposed by Ren *et al.* in [40] to make the number of Kraus operators in each channel equal. We then use the same procedure as in Example 3. When $\alpha = \frac{1}{3}$ and $p = 0.7$, one can see that for some cases the lower bounds \overline{LB}_3 and \overline{LB}_4 are superior, whereas for some cases the lower bounds \overline{LB}_1 and \overline{LB}_2 are larger, which is illustrated in FIG. 4.

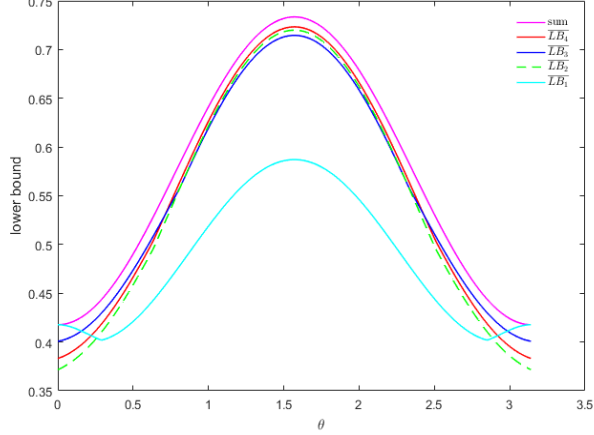


FIG. 3: Set $\alpha = \frac{1}{3}$ and $p = 0.7$. The magenta line represents the value of $I_\rho^{\frac{1}{3}}(\Lambda) + I_\rho^{\frac{1}{3}}(\varepsilon) + I_\rho^{\frac{1}{3}}(\phi)$; the red line represents our lower bound \overline{LB}_4 ; the blue line represents our lower bound \overline{LB}_3 ; the green dashed line represents the lower bound \overline{LB}_2 ; the cyan line represents the lower bound \overline{LB}_1 . Obviously, our lower bound \overline{LB}_4 is always tighter than the lower bound \overline{LB}_2 . The lower bounds \overline{LB}_3 and \overline{LB}_4 are superior for some θ , whereas the lower bound \overline{LB}_1 is larger for some θ .

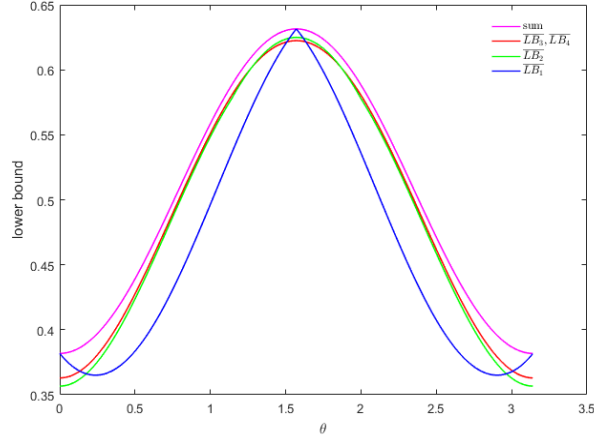


FIG. 4: Set $\alpha = \frac{1}{3}$ and $p = 0.7$. The magenta line represents the value of $I_\rho^{\frac{1}{3}}(\Lambda) + I_\rho^{\frac{1}{3}}(\varepsilon) + I_\rho^{\frac{1}{3}}(U)$; the red line represents our lower bounds \overline{LB}_3 and \overline{LB}_4 ; the green line represents the lower bound \overline{LB}_2 ; the blue line represents the lower bound \overline{LB}_1 . One can see that for some θ the results obtained by us are tighter, but for some θ the lower bounds \overline{LB}_1 and \overline{LB}_2 are superior.

V. CONCLUSION

To sum up, we have obtained the new sum uncertainty relations based on metric-adjusted skew information for arbitrary finite n observables and arbitrary finite N quantum channels. Furthermore, the sum uncertainty relations with respect to Wigner-Yanase-Dyson skew information were provided, and we gave several examples to confirm our results are better than the lower bounds in [40]. Moreover, the sum uncertainty relations in this paper are consistent with the results in [9] with regarding to Wigner-Yanase skew information for finite observables, namely, the conclusions we have drawn cover the results in [9]. May our results provide a reference for future work on the study of sum uncertainty relations.

ACKNOWLEDGMENTS

This work was supported by the National Natural Science Foundation of China under Grant No. 12071110, the Hebei Natural Science Foundation of China under Grant No. A2020205014, and funded by Science and Technology Project of Hebei Education Department under Grant Nos. ZD2020167, ZD2021066.

[1] W. Heisenberg, Über den anschaulichen Inhalt der quantentheoretischen Kinematik und Mechanik, *Z. Phys.* **43**, 172-198 (1927).

[2] H. P. Robertson, The uncertainty principle, *Phys. Rev.* **34**, 163 (1929).

[3] E. Schrödinger, Probability relations between separated systems, *Proc. Camb. Phil. Soc.* **32**, 446-452 (1936).

[4] L. Maccone and A. K. Pati, Stronger uncertainty relations for all incompatible observables, *Phys. Rev. Lett.* **113**, 260401 (2014).

[5] K. K. Wang, X. Zhan, Z. H. Bian, J. Li, Y. S. Zhang, and P. Xue, Experimental investigation of the stronger uncertainty relations for all incompatible observables, *Phys. Rev. A* **93**, 052108 (2016).

[6] D. Mondal, S. Bagchi, and A. K. Pati, Tighter uncertainty and reverse uncertainty relations, *Phys. Rev. A* **95**, 052117 (2017).

[7] Q. C. Song, J. L. Li, G. X. Peng, and C. F. Qiao, A stronger multi-observable uncertainty relation, *Sci. Rep.* **7**, 44764 (2017).

[8] J. Zhang, Y. Zhang, and C. S. Yu, Stronger uncertainty relations with improvable upper and lower bounds, *Quantum Inf. Process.* **16**, 131 (2017).

[9] Q. H. Zhang and S. M. Fei, Tighter sum uncertainty relations via variance and Wigner-Yanase skew information for N incompatible observables, *Quantum Inf. Process.* **20**, 384 (2021).

[10] D. Deutsch, Uncertainty in quantum measurements, *Phys. Rev. Lett.* **50**, 631 (1983).

[11] H. Maassen and J. B. M. Uffink, Generalized entropic uncertainty relations, *Phys. Rev. Lett.* **60**, 1103 (1988).

[12] I. B. Birula, Formulation of the uncertainty relations in terms of the Rényi entropies, *Phys. Rev. A* **74**, 052101 (2006).

[13] G. Wilk and Z. Włodarczyk, Uncertainty relations in terms of the Tsallis entropy, *Phys. Rev. A* **79**, 062108 (2009).

[14] M. Tomamichel and R. Renner, Uncertainty relation for smooth entropies, *Phys. Rev. Lett.* **106**, 110506 (2011).

[15] H. J. Mu and Y. M. Li, Quantum uncertainty relations of two quantum relative entropies of coherence, *Phys. Rev. A* **102**, 022217 (2020).

[16] P. J. Coles and M. Piani, Improved entropic uncertainty relations and information exclusion relations, *Phys. Rev. A* **89**, 022112 (2014).

[17] Y. H. Zhou, Z. W. Yu, and X. B. Wang, Making the decoy-state measurement-device-independent quantum key distribution practically useful, *Phys. Rev. A* **93**, 042324 (2016).

[18] C. F. Li, J. S. Xu, X. Y. Xu, K. Li, and G. C. Guo, Experimental investigation of the entanglement-assisted entropic uncertainty principle, *Nat. Phys.* **7**, 752-756 (2011).

[19] T. Gao, F. L. Yan, and S. J. van Enk, Permutationally invariant part of a density matrix and nonseparability of N -qubit states, *Phys. Rev. Lett.* **112**, 180501 (2014).

[20] M. L. Hu and H. Fan, Quantum-memory-assisted entropic uncertainty principle, teleportation, and entanglement witness in structured reservoirs, *Phys. Rev. A* **86**, 032338 (2012).

[21] J. Schneeloch, C. J. Broadbent, S. P. Walborn, E. G. Cavalcanti, and J. C. Howell, Einstein-Podolsky-Rosen steering inequalities from entropic uncertainty relations, *Phys. Rev. A* **87**, 062103 (2013).

[22] M. Jarzyna and R. D. Dobrzański, True precision limits in quantum metrology, *New J. Phys.* **17**, 013010 (2015).

[23] S. L. Luo, Wigner-Yanase skew information and uncertainty relations, *Phys. Rev. Lett.* **91**, 180403 (2003).

[24] E. P. Wigner and M. M. Yanase, Information contents of distributions, *Proc. Natl. Acad. Sci. USA* **49**, 910-918 (1963).

[25] E. H. Lieb, Convex trace functions and the Wigner-Yanase-Dyson conjecture, *Adv. Math.* **11**, 267-288 (1973).

[26] E. H. Lieb and M. B. Ruskai, A fundamental property of quantum-mechanical entropy, *Phys. Rev. Lett.* **30**, 434 (1973).

[27] S. L. Luo and Q. Zhang, On skew information, *IEEE Trans. Inf. Theory* **50**, 1778-1782 (2004).

[28] S. L. Luo, Wigner-Yanase skew information vs. quantum Fisher information, *Proc. Am. Math. Soc.* **132**, 885-890 (2004).

[29] P. Gibilisco, D. Imparato, and T. Isola, Inequalities for quantum Fisher information, *Proc. Am. Math. Soc.* **137**, 317-327 (2009).

[30] D. Petz, Monotone metrics on matrix spaces, *Linear Algebra Appl.* **244**, 81-96 (1996).

[31] F. Hansen, Metric adjusted skew information, *Proc. Natl. Acad. Sci. USA* **105**, 9909-9916 (2008).

[32] H. F. Hofmann and S. Takeuchi, Violation of local uncertainty relations as a signature of entanglement, *Phys. Rev. A* **68**, 032103 (2003).

[33] O. Gühne, Characterizing entanglement via uncertainty relations, *Phys. Rev. Lett.* **92**, 117903 (2004).

[34] N. Li and S. L. Luo, Entanglement detection via quantum Fisher information, *Phys. Rev. A* **88**, 014301 (2013).

[35] Y. Hong, X. F. Qi, T. Gao, and F. L. Yan, Detection of multipartite entanglement via quantum Fisher information, *Europhys. Lett.* **134**, 60006 (2021).

[36] J. Li and L. Chen, Detection of genuine multipartite entanglement based on uncertainty relations, *Quantum Inf. Process.* **20**, 220 (2021).

- [37] L. M. Zhang, T. Gao, and F. L. Yan, Tighter uncertainty relations based on Wigner-Yanase skew information for observables and channels, *Phys. Lett. A* **387**, 127029 (2021).
- [38] Q. H. Zhang, J. F. Wu, and S. M. Fei, A note on uncertainty relations of arbitrary N quantum channels, *Laser Phys. Lett.* **18**, 095204 (2021).
- [39] L. Cai, Sum uncertainty relations based on metric-adjusted skew information, *Quantum Inf. Process.* **20**, 72 (2021).
- [40] R. N. Ren, P. Li, M. F. Ye, and Y. M. Li, Tighter sum uncertainty relations based on metric-adjusted skew information, *Phys. Rev. A* **104**, 052414 (2021).